AMERICAN SOCIETY FOR MICROBIOLOGY | Journal of Virology

Antibody Binding Modulates Conformational Exchange in Domain III of Dengue Virus E Protein

Adolfo H. Moraes,[a] Luca Simonelli,[b] Mattia Pedotti,[b] Fabio C. L. Almeida,[a] Luca Varani,[b] Ana P. Valente[a]

National NMR Center CNRMN, Federal University of Rio de Janeiro, Rio de Janeiro, Brazil[a]; Institute for Research in Biomedicine, Università della Svizzera Italiana (USI), Bellinzona, Switzerland[b]

ABSTRACT

Domain III of dengue virus E protein (DIII) participates in the recognition of cell receptors and in structural rearrangements required for membrane fusion and ultimately viral infection; furthermore, it contains epitopes for neutralizing antibodies and has been considered a potential vaccination agent. In this work, we addressed various structural aspects of DIII and their relevance for both the dengue virus infection mechanism and antibody recognition. We provided a dynamic description of DIII at physiological and endosomal pHs and in complex with the neutralizing human antibody DV32.6. We observed conformational exchange in the isolated DIII, in regions important for the packing of E protein dimers on the virus surface. This conformational diversity is likely to facilitate the partial detachment of DIII from the other E protein domains, which is required to achieve fusion to the host cellular membranes and to expose the epitopes of many anti-DIII antibodies. A comparison of DIII of two dengue virus serotypes revealed many common features but also some possibly unexpected differences. Antibody binding to DIII of dengue virus serotype 4 attenuated the conformational exchange in the epitope region but, surprisingly, generated exchange in other parts of DIII through allosteric effects.

IMPORTANCE

Many studies have provided extensive structural information on the E protein and particularly on DIII, also in complex with antibodies. However, there is very scarce information regarding the molecular dynamics of DIII, and almost nothing is available on the dynamic effect of antibody binding, especially at the quantitative level. This work provides one of the very rare descriptions of the effect of antibody binding on antigen dynamics.

Dengue virus (DENV) is a member of the *Flaviviridae* family, which includes yellow fever, West Nile, Japanese tick-borne encephalitis, and other viruses. DENV is responsible for ~500,000 hospitalizations and >20,000 deaths per year (1). The incidence and geographic expansion of the virus are constantly increasing, and no cure or licensed vaccine is currently available for Dengue disease. There are four Dengue virus serotypes, DENV1 to -4, and secondary infection with a different serotype is associated with a severe form of the disease: dengue hemorrhagic fever (2). This is probably facilitated by a process called antibody-dependent enhancement (ADE), where cross-reactive, poorly neutralizing antibodies allow infection of Fc receptor-bearing cells, leading to increased viral loads and infectivity (3).

Flaviviruses recognize their target cells via the interaction of glycoprotein E (E protein) with host receptors, which include the extracellular matrix components (4–6). After virus internalization by endocytosis, exposure to the lower endosomal pH leads to alterations of the E protein structure, exposing the fusion peptide and allowing it to interact with the endosome membrane and mediate viral fusion (1, 7–9).

The virus surface is formed by 180 units of antiparallel E protein dimers (1, 7, 10, 11). Crystal structures showed that the ectodomain of E is formed by three domains (domain I [DI], DII, and DIII): DII contains the main dimerization interface, glycosylation sites, and the fusion peptide. DIII, in the C-terminal region of E, covers the fusion peptide of a neighboring dimer molecule and is linked to DI by a loop that mediates a large interdomain rearrangement during the cell membrane fusion process. DIII is also supposedly involved in host cell receptor recognition. This domain adopts an immunoglobulin-like fold with six β-strands forming two β-sheets (ABD and CEF) (12–14). The structure is well conserved among DENV serotypes and other flaviviruses, despite DIII being the region with the highest sequence variability. The E protein is the target of many neutralizing antibodies and a major component of the natural immune response to dengue virus (15–18). Antibodies against DIII have been shown to be potent but not broad neutralizers, supposedly due to such variability.

Conformational flexibility on the E protein plays a significant role in antibody recognition (19). Indeed, all DIII antibodies with a known structure recognize epitopes that are only partially accessible on the mature viral surface (20). This might explain why none of these antibodies is particularly potent, since virus binding probably requires relatively rare structural motions which briefly expose the epitopes. Cryo-electron microscopy (cryo-EM) and X-ray crystallography showed different E protein conformations when bound by an antibody, suggesting that the antibody can either induce a conformational change in the E protein or select an existing, albeit rare, conformation.

The data described above suggest that not only the primary

Received 10 September 2015 **Accepted** 25 November 2015

Accepted manuscript posted online 4 December 2015

Citation Moraes AH, Simonelli L, Pedotti M, Almeida FCL, Varani L, Valente AP. 2016. Antibody binding modulates conformational exchange in domain III of dengue virus E protein. J Virol 90:1802–1811. doi:10.1128/JVI.02314-15.

Editor: M. S. Diamond

Address correspondence to Luca Varani, luca.varani@irb.usi.ch, or Ana P. Valente, valente@cnrmn.bioqmed.ufrj.br.

sequence and tertiary structure but also differences in molecular dynamics occurring on the DENV surface can impact epitope accessibility, binding, and, consequently, the neutralization properties and serotype specificity of antibodies. Despite DIII being considered an attractive target for both vaccine and antiviral design (21–26), the effects of its atomic-level motions on the molecular mechanisms leading to virus infection and antibody recognition have been largely neglected. Indeed, antibody-antigen structures are usually explored by X-ray crystallography, which, by its own nature, tends to overlook dynamic effects.

In this work, we studied the structure and molecular dynamics of DIII, highlighting their role in the molecular mechanisms of virus infection and antibody recognition. Using a combination of nuclear magnetic resonance (NMR) experiments, we characterized, at the residue level, the motion of DIII free in solution, at different pHs, and in complex with a neutralizing human antibody.

MATERIALS AND METHODS

Dengue virus DIII and DV32.6 single-chain variable-fragment (scFv) antibody production and purification. DIII from the E protein of each DENV serotype was expressed in *Escherichia coli* Rosetta cells with a pET21 vector (Novagen) in M9 minimal medium, using aptly labeled nutrients (NH_4Cl and glucose) as the sole sources of nitrogen and carbon, as described previously (27).

The DV32.6 single-chain antibody was expressed in *E. coli* Rosetta cells with a pET21 vector (Novagen) in LB medium. The cells were harvested 5 h after induction, which was done at an optical density at 600 nm (OD_{600}) of 0.7. After sonication and centrifugation, the pellet was repeatedly washed and centrifuged in a solution containing 50 mM morpholineethanesulfonic acid (MES) (pH 6.5), 100 mM NaCl, 0.5 mM dithiothreitol (DTT), and 1% Triton X-100. The pellet was finally resuspended in a solution containing 50 mM MES (pH 6.5), 6 M guanidinium chloride, and 1 M NaCl (solubilization buffer). Following the addition of 0.2% polyethyleneimine (PEI) and centrifugation, 65% ammonium sulfate was added to the supernatant. After centrifugation, the pellet was resuspended in solubilization buffer and loaded onto a HiTrap chelating column (GE). Finally the eluted sample was refolded in a solution containing 20 mM NaP (pH 7.5), 100 mM NaCl, 200 mM arginine, 1 mM reduced glutathione, and 0.1 mM oxidized glutathione for 18 h at 4°C; concentrated with Vivaspin concentrators (Sartorius); and further purified on a Superdex-75 size exclusion column (GE) with the buffer used for NMR spectroscopy.

NMR spectroscopy. NMR experiments were carried out on Bruker Avance III 800-MHz spectrometer equipped with a 5-mm triple-resonance probe and on a Bruker Avance III 600-MHz spectrometer equipped with a 5-mm triple-resonance cryogenic probe. The ^{1}H-^{15}N heteronuclear single quantum coherence (HSQC) spectra of DIII of DENV1 (DIII-1) and DENV4 (DIII-4) were assigned by using NMR chemical shifts deposited in the Biological Magnetic Resonance Bank (BMRB; http://www.bmrb.wisc.edu) (accession numbers 15782 for DIII-1 and 7082 for DIII-4). Triple-resonance experiments were performed to complete the assignment of DIII-4 by using 260 μM ^{15}N,^{13}C-labeled DIII-4 in a solution containing 20 mM phosphate buffer (pH 6.0) and 50 mM NaCl at 308 K. All data from NMR experiments were processed by using Topspin 2.1 (Biospin; Bruker) and NMRpipe (28) and analyzed with the program CCPN (29).

Molecular dynamics of DIII-1 and DIII-4 from NMR relaxation experiments. The backbone molecular dynamics of DIII-1 and DIII-4 were characterized by ^{15}N-NMR relaxation experiments using 260 μM DIII-1 and DIII-4 at 308 K. ^{15}N R_1 (longitudinal) and R_2 (transversal) relaxation rates were obtained by fitting the intensities of NMR peaks in spectra acquired with different delay times. In R_1 experiments, delay times of 50, 100, 200, 300, 400, 600, 800, 1,000, and 1,500 ms were used. Values of 17, 34, 51, 85, 119, 135, 159, 170, 203, and 237 ms were used to calculate R_2 ratios. ^{1}H-^{15}N steady-state heteronuclear nuclear Overhauser effects (NOE) were calculated from peak intensities in spectra acquired with and without saturation of amide protons (30–32). The relaxation rates were analyzed with reduced spectral density formalism (33, 34), using the program Relax (35, 36), and with the theoretical formalism of Lipari and Szabo (37), using the program Tensor 2.0 (38). The diffusion correlation time, τ_c, which reflects the global tumbling of the protein, was calculated from the R_2/R_1 ratio by using the isotropic diffusion model. Residues showing R_2 values higher than the average plus the standard deviation and NOE values lower than 0.65 were excluded from the analysis. Diffusion tensors were also calculated by using the axial symmetric diffusion model. This model was used for calculating the internal molecular dynamics parameters order parameter, S^2, and conformational exchange ratio, R_{ex} (per second), which reflects movements of the N—H bond in picosecond-to-nanosecond and microsecond-to-millisecond time scales, respectively.

The molecular dynamics of DIII-1 and DIII-4 complexed with scFv was also analyzed by using R_1 and R_2 ratios. Data in the experiments were acquired by using delay times of 50, 100, 200, 300, 500, 700, and 900 ms for R_1 and 17, 34, 51, 68, 85, and 119 ms for R_2.

pH variation NMR experiments. The effect of pH variation from 5.5 to 7.2 on the structure of DIII-4 was assessed by chemical shift perturbation of amide ^{1}H and ^{15}N obtained from ^{1}H-^{15}N HSQC experiments carried out at both pHs. The chemical shift perturbation (CSP) index was calculated by using the formula: $CSP = \sqrt{(\Delta H)^2 + 0.1(\Delta N)^2}$ here, ΔH and ΔN are the chemical shift differences in the ^{1}H and ^{15}N dimensions, respectively. The transversal relaxation rates, R_2, of amide ^{15}N of DIII-4 were also calculated to monitor the molecular dynamics changes caused by pH variation. In these experiments, the same delay time values mentioned above for the Lipari-Szabo analysis were used. All experiments were performed by using 100 μM DIII-4 in a solution containing 20 mM phosphate buffer, 2 mM sodium azide, and 50 mM NaCl at 35°C.

Binding of DIII-1 and DIII-4 with scFv DV32.6. The binding of scFv DV32.6 to DIII-1 and DIII-4 was monitored by using the chemical shift perturbation index of amide ^{1}H and ^{15}N obtained from comparison of the HSQC spectra of DIII free and in complex with scFv32.6. The CSP index was calculated with the same formula mentioned above for pH variation experiments. All binding experiments were performed by using 260 μM DIII-1 and -4 and 260 μM DV32.6 in a solution containing 20 mM phosphate buffer, 2 mM sodium azide, and 50 mM NaCl (pH 6.0) at 35°C.

Paramagnetic relaxation enhancement experiments. To monitor the solvent accessibility of residues of DIII-4 in complex with scFv DV32.6, ^{1}H-^{15}N HSQC NMR spectra of ^{15}N isotopically labeled DIII-4 in complex with scFv DV32.6 were recorded in the presence and in the absence of the gadolinium-based paramagnetic relaxation agent Gd-diethylenetriamine pentaacetic acid-bismethylamide [Gd(DTPA-BMA)] (GE Life Science, Little Chalfont, United Kingdom). The effect of Gd(DTPA-BMA) on the relaxation rates of the amide ^{15}N nucleus of the DIII-4–scFv DV32.6 complex was assessed by calculating the difference in the intensities of NMR resonance on the ^{1}H-^{15}N HSQC of the complex upon the addition of aliquots of 1 to 10 mM the relaxation agent. In Fig. 2B, the difference in intensity is denoted as Int − Int(Gad). Experiments were performed with 200 μM DIII-4 and 200 μM DV32.6 in a solution containing 20 mM phosphate buffer, 2 mM sodium azide, and 50 mM NaCl (pH 6.0) at 35°C.

RESULTS

Comparative molecular dynamics of DIII-1 and DIII-4 determined by NMR spectroscopy. We used solution NMR spectroscopy to characterize the molecular dynamics of E protein DIII at the residue level. NMR is possibly the only experimental technique that can provide a quantitative measure of residue flexibility. The general idea is that the rate of NMR signal decay (relaxation) is related to the flexibility of the atoms observed (39, 40). In this work, we used standard NMR pulse sequences to measure ^{15}N R_1, R_2, and NOE rates. The global rotational diffusion and internal movements of ^{1}H-^{15}N bonds in DIII were characterized by using both Lipari-Szabo formalism and the reduced spectral density

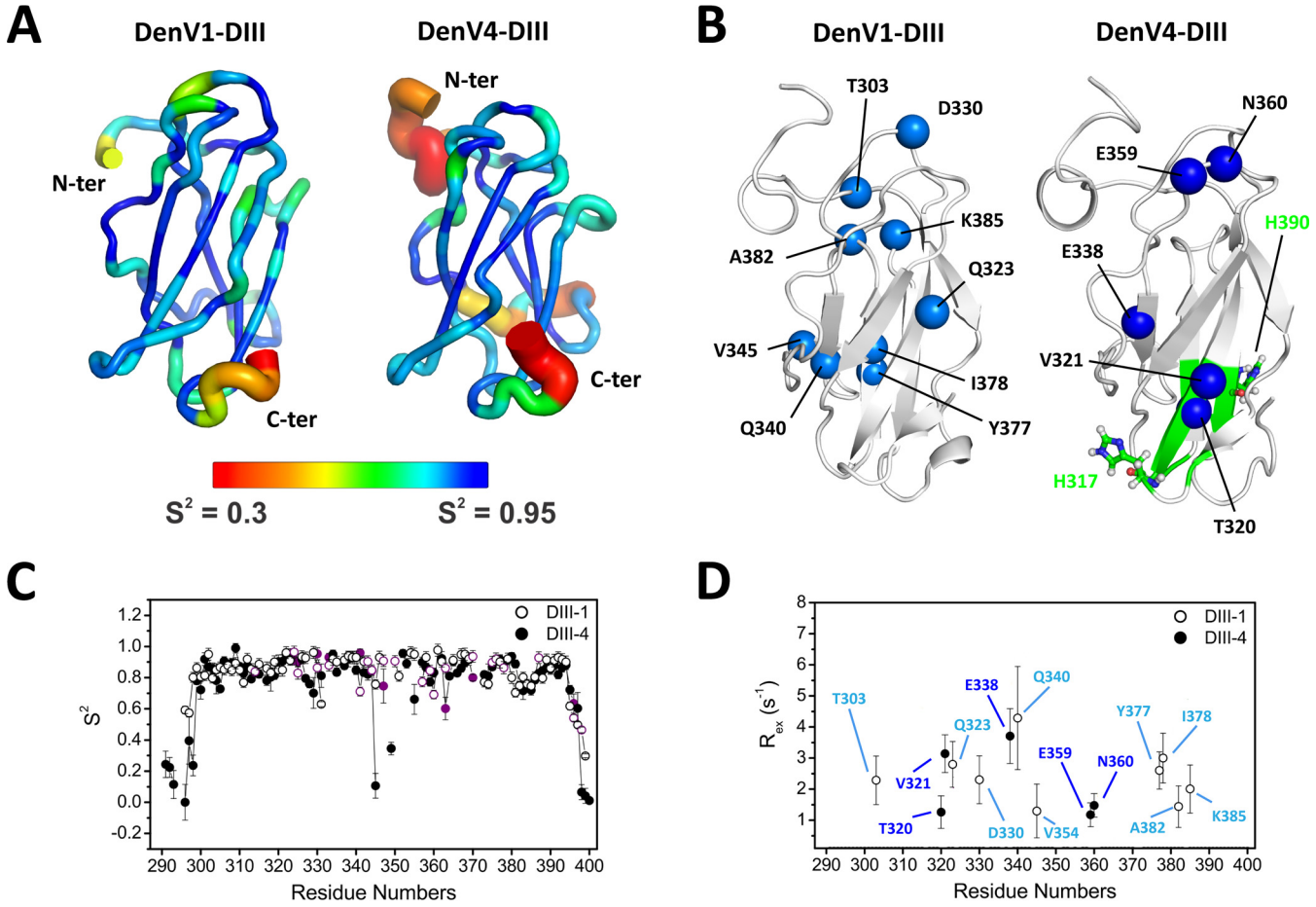

FIG 1 Flexibility of DIII of dengue virus E protein. (A) Ribbon representation of DIII of serotypes 1 (left) and 4 (right). Backbone flexibility is indicated by ribbon thickness and color. Blue and thin ribbons represent rigidity, whereas red and thick ribbons indicate residues with increased motion. The values for the order parameter S^2 are shown on the structure. S^2 is derived from NMR experiments; values range from 0 to 1, with lower values indicating increasing flexibility. (B) Cartoon representation of DIII, with residues showing conformational exchange in free DIII indicated as light (DIII-1) and dark (DIII-4) blue spheres. Residues experiencing a different chemical environment at low pH, according to NMR mapping experiments, are shown in green on the structure of DIII-4. (C) Values for the order parameter S^2 shown on the structure in panel A are plotted as a function of residue number, and residues with signal overlap are shown in purple. (D) NMR-derived R_{ex} values indicating conformational exchange plotted as a function of residue number.

function. Overall, the data allowed us to draw a comprehensive picture of the dynamic properties of DIII.

A first indication about the experimental reliability is obtained from the correlation times (τ_c), which depend on the rate at which molecules tumble in solution. Values for DIII-1 and DIII-4 were 6.1 and 5.7 ns, respectively, using an isotropic model for molecular rotational diffusion. These values are consistent with the tumbling of proteins with a molecular mass of ~10 kDa, such as DIII. Parallel and perpendicular components of the rotational diffusion tensor, $D_{//}$ and $D\perp$, of 2.5 and 3.0 ns for DIII-1 and 2.8 and 3.1 ns for DIII-4, respectively, were obtained using axially symmetric anisotropic diffusion models.

Flexibility within a given residue can be investigated via the so-called order parameter (S^2) and spectral density function $J(\omega_{15N})$. Results for backbone NH atoms show similar behaviors for DIII-1 and DIII-4. Residues in the N and C termini presented higher flexibility, as indicated by lower $J(\omega_{15N})$ and S^2 values, as expected for isolated domain fragments. Some residues located in loops BC, CD, and EF also showed a higher degree of flexibility than residues in the beta strands (Fig. 1A and C). Despite the similarity observed in the picosecond-to-nanosecond time scale, DIII-1 and DIII-4 showed many differences when slower movements (microsecond-to-millisecond time scale) were taken into account. These slower movements typically indicate exchange between alternative conformations. Analysis of the exchange rate, R_{ex} (Fig. 1B and D), and $J(0)$ show contributions from exchange in the microsecond-to-millisecond time scale, indicated by higher-than-average values. Residues showing conformational exchange are indicated by spheres in Fig. 1B.

Intriguingly, the residues with conformational exchange mapped to different parts of the structure in the two serotypes.

Another difference is related to V320, which presented duplicate resonances in DIII-1, typically related to a slow conformational exchange regime in the NMR chemical shift time scale. The corresponding residue of DIII-4, T320, instead showed a lower signal intensity, which is a typical consequence of line broadening caused by conformational exchange at the fast-to-intermediate scale (not shown). Residue 320, in other words, can experience different conformations in both DIII-1 and DIII4, but the rates at which it alternates between such conformations appear different in the two cases.

In order to quantify the conformational exchange identified in DIII, we used Carr-Purcell-Meiboom-Gill (CPMG) relaxation dispersion NMR spectroscopy (41, 42). $R_{2,\mathrm{eff}}$ values obtained from ^{15}N CPMG experiments at 298 K, 303 K, and 308 K showed no significant difference between the $R_{2,\mathrm{eff}}$ values measured with CPMG frequencies of 50 and 1,000 Hz, meaning that the residues have a $K_{ex}/\Delta\omega$ value of $\gg 1$, or a K_{ex} value of $\gg$2,000 Hz, outside the time scale range in which it is possible to separate kinetics, thermodynamics, and chemical shift parameters by fitting the experimental data with theoretical models (43–45).

The DENV E protein undergoes a profound conformational change after cell entry, when the pH drops from 7 to ~5 in the endosome. Although the overall fold of DIII remains identical, its position changes by ~70° in relation to the other E protein domains (13, 46, 47). This process involves disruption of specific interactions between DI and DIII of the E monomer. In particular, at high pH, E368 on DIII forms electrostatic interactions with R9 in DI, whereas it interacts with H317 of DIII at low pH. Although we observed DIII only in the absence of the other domains and thus cannot assess the impact of interactions between different domains or different E protein dimers on the virus surface, it is still instructive to compare its behavior at decreasing pHs.

The structural changes in DIII-4 caused by pH variation were monitored by NMR mapping experiments, measuring the deviations of chemical shifts in ^{1}H-^{15}N HSQC NMR spectra. Briefly, the chemical shift is extremely sensitive to the local chemical environment; chemical shift changes therefore indicate local structural or chemical alterations. Analysis of the CSP index calculated from experiments carried out at pH 5.5 and pH 7.2 indicates the residues affected by pH variation (Fig. 1B, green). The residues cluster in the DIII region close to the neighboring E protein dimer as well as around H390 in DIII-4 (residues 315, 317 to 321, 376, 377, 390, and 391). No significant differences between DIII-1 and DIII-4 were noted, which might not be surprising considering that the pH-dependent mechanism for E protein rearrangement is likely conserved among serotypes. Despite the chemical shift changes showing clear differences, the molecular motions of DIII-4 at pH 5.5 and pH 7.2 were very similar, as measured by the transversal relaxation rates, R_2. Thus, the flexibility of the isolated DIII-4 is not affected by pH variation.

Interaction of DIII with antibody DV32.6. Binding of the neutralizing human antibody DV32.6 to DIII of each serotype was previously observed by NMR spectroscopy (27); however, a 50-kDa Fab version of the antibody (48) was used, whereas in this work, we used a 25-kDa single-chain version. Our first task, therefore, was to repeat the NMR mapping experiments to verify that the two antibody fragments behave similarly. Indeed, there is very good agreement among the data collected, with the difference that the scFv fragment, of a lower molecular mass, provides higher-quality NMR spectra.

The binding and mapping of residues of DIII-1 and DIII-4 affected by complex formation were monitored by NMR chemical shift mapping (47). Briefly, the chemical environment of DIII epitope residues changes upon antibody binding, and so does the position of their NMR signal (chemical shift). Residues with significant chemical shift differences between free DIII and DIII bound to the antibody are therefore identified as being part of the intermolecular interface. Several DIII residues showed large chemical shift variations in ^{1}H-^{15}N HSQC NMR spectra upon antibody binding, delimiting a contiguous and well-defined region (Fig. 2 and 3, purple). Other residues, for instance, E311 in DIII-1, showed broadening and weak intensity upon binding, a strong indication of conformational exchange in the microsecond-to-millisecond time scale induced by complex formation. As noted previously (27), NMR mapping showed that the antibody epitope is only partially accessible on the X-ray structure of the full E protein, being covered by residues from the other domains in the neighboring E monomer (Fig. 2C and D) (11).

To further characterize the epitope and to be able to distinguish the residues that are directly involved in antibody interactions from residues that are allosterically affected by antibody binding, we probed the accessibility of DIII residues by a small paramagnetic molecule. We monitored the effect of the addition of the gadolinium-based paramagnetic relaxation agent Gd(DTPA-BMA) on NMR relaxation. Gd(DTPA-BMA) is uncharged and highly soluble in water and presents low specific binding to proteins (49). It is expected to enhance the relaxation rates and thus decrease the NMR peak intensity of the protein amide groups that are exposed to water and are therefore at the protein surface. Interface residues in the antibody-DIII complex are not solvent accessible, and their signal is thus not disturbed by the presence of the paramagnetic probe. By comparing the ^{1}H-^{15}N HSQC signal intensities of the antibody-DIII complex in the presence and absence of the paramagnetic molecule, it is possible to distinguish interface DIII residues (signal intensity not altered by gadolinium) from residues affected by antibody binding (previously identified by chemical shift mapping) but not directly located at the interface (lower intensity in the presence of the paramagnetic agent). Results are shown in Fig. 2.

In general, a very good correlation was found between the CSP index and the degree of protection against the decrease of intensity caused by Gd(DTPA-BMA) in solution. Results show that many epitope residues mapped by CSP are protected from Gd (i.e., the difference in intensities with and without Gd is zero). On the other hand, epitope residues such as S353, T388, and W391 (Fig. 2B) have a significant decrease in intensity in the presence of Gd, suggesting that they are not directly located at the antibody-antigen interface, but they are probably related to allosteric effects following binding. Indeed, these residues are on the opposite face of DIII-4, away from the antibody-binding site.

Backbone dynamics of DIII in complex with antibody DV32.6. We analyzed the impact of antibody binding on the flexibility of DIII by comparing the ratio of ^{15}N relaxation rates, R_2 and R_1, in the presence or absence of antibody DV32.6.

The average R_2/R_1 ratio values were ~4.5 s^{-1} for the free DIII domains and ~22 s^{-1} for DIII-antibody complexes, reflecting the higher molecular mass of the complex. With regard to internal molecular dynamics, binding of scFv DV32.6 to DIII-1 led to a decrease of intensity beyond detection for residues E311, T315, T321, and Q323 located in the β-sheet (ABD); I335 in the BC loop; and E370 and E375 in the β-sheet (CEF). Residues T339, N355, and Y377 also showed higher-than-average R_2/R_1 ratio values. Both effects are a strong indication of changes in the conformational exchange regime upon binding.

Comparison of the R_2/R_1 ratios for free DIII-4 and DIII-4 in complex with scFv DV32.6 indicates that residues V321, E338, and N360 are in conformational exchange in free DIII-4 but not in the complex. This could be interpreted as a stabilization of the conformation around those residues induced by antibody binding. Residues V321 and E338 are part of the NMR-characterized

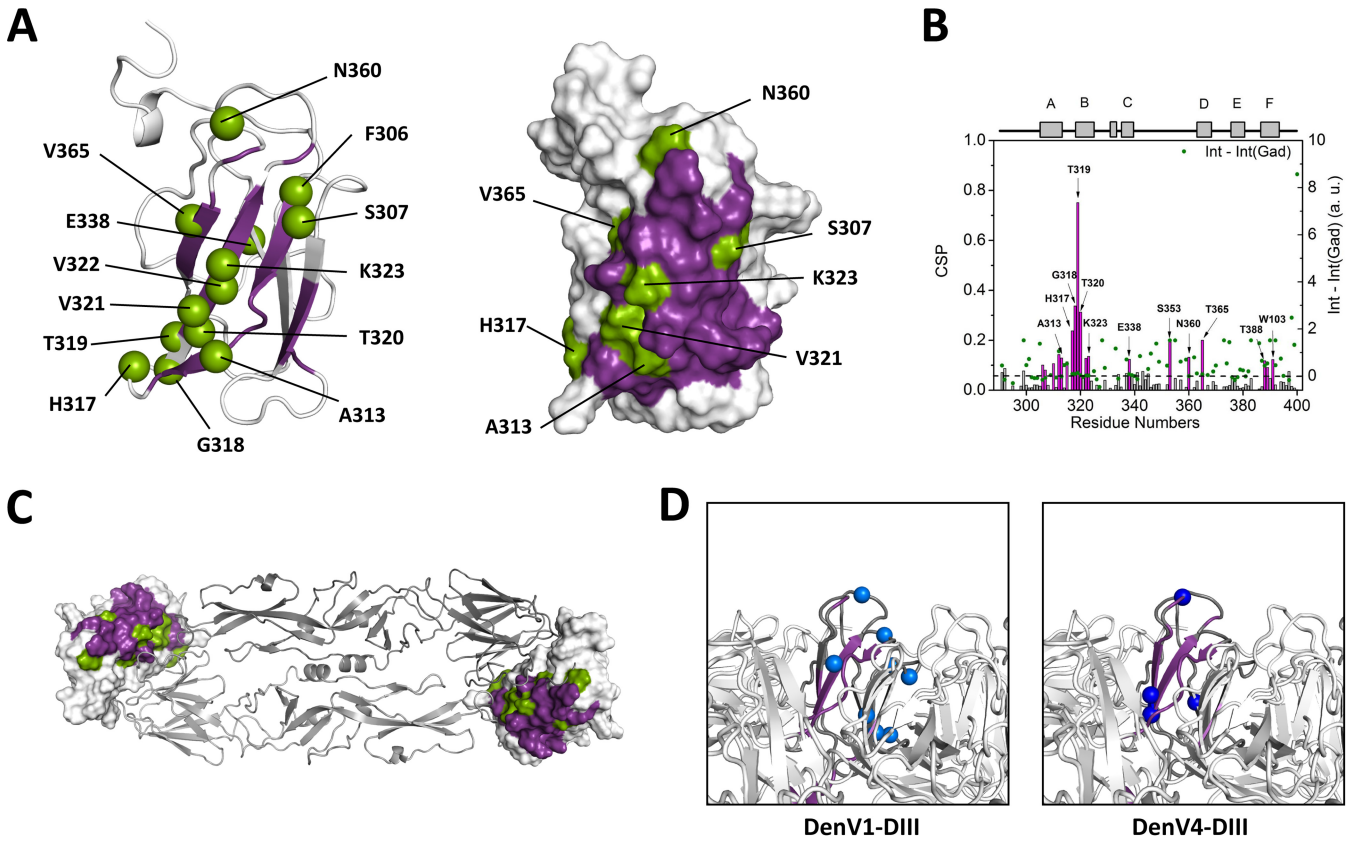

FIG 2 Binding site of antibody DV32.6 on DIII. (A and C) DIII-4 residues affected by antibody binding according to NMR mapping experiments are shown in purple on the cartoon and surface representation of isolated DIII-4 (A) and on the structure of the full E protein dimer (C). The epitope is only partially accessible in the context of the dimer. Antigen residues directly located at the intermolecular interface and not accessible to a paramagnetic molecular probe are shown in green. (B) NMR data used to generate panels A and C, where the CSP index (left scale) is shown as vertical bars versus residue number. A higher CSP index indicates that a given residue is affected by antibody binding, shown in purple in the chart. Residues directly located at the antibody-antigen interface were identified by probing their accessibility by a small paramagnetic molecular probe. Right scale shows the difference of intensity in the HSQC spectra of the complex without or with Gd(DTPA-BMA). Results of this experiment are represented by green circles. Residues with values close to zero (right scale) (the zero value is indicated by a dotted line) are not accessible to the probe and thus are located either inside the protein or at the intermolecular interface. a.u., arbitrary units. (D) Cartoon representation of part of the dengue virus surface. The epitope of DV32.6 is shown in purple on DIII. The epitope is mostly inaccessible on the virus surface, suggesting that antibody binding requires conformational rearrangement. Antigen residues that show conformational exchange in the free antigen are shown as blue spheres, as described in the legend of Fig. 1.

epitope and are directly involved in antibody binding (Fig. 2), so it is not surprising that they change the conformational equilibrium and become more ordered in the complex due to intermolecular interactions. In contrast, residues A358, V364, and N366 broaden beyond detection in the complex. Also, residues E327 and L357 appear to contribute to conformational exchange in the antibody-DIII complex but not in free DIII. These residues are highlighted in the structure of DIII shown in Fig. 3 (yellow and orange).

Taken together, these data suggest that on one hand, antibody binding reduces the conformational freedom of epitope residues, which is not surprising, but that on the other hand, it provokes allosteric conformational effects on DIII that are not limited to the stabilization of conformational exchange or conformational selection in the antigen.

It is worth noting that residues of DIII-1 that are involved in conformational exchange processes in the complex are localized on both faces of the DIII structure (β-sheets ABD and CEF) (Fig. 3A). In contrast, in the DIII-4–DV32.6 complex, residues showing movements in the microsecond-to-millisecond time scale are localized on the protein side formed by β-sheet ABD and loops BC and CD (Fig. 3D). These results indicate not only that DIII-1 and DIII-4 present different degrees of motion in the microsecond-to-millisecond time scale but also that different residues are affected by antibody binding in the two serotypes, suggesting that the molecular dynamics of the DIII-1 and DIII-4 complexes with DV32.6 are also different.

DISCUSSION

The importance of protein flexibility in structure and intermolecular interactions has been recognized in several works (44, 50, 51). Little has been done, however, to investigate the role of molecular motions in antibody-antigen recognition despite the attention that these complexes receive in several research fields. One of the reasons for the lack of available data is that antibody-antigen complexes are large and not easily accessible by solution NMR spectroscopy, the main tool that allows residue-level, quantitative analysis of protein dynamics.

Antibodies interact with antigens through six "CDR loops" with lengths typically up to 20 residues. Flexibility in these loops might confer broad selectivity to an antibody, i.e., the ability to recognize and bind different antigens (e.g., virus serotypes), possibly at the price of higher entropic costs if these loops become

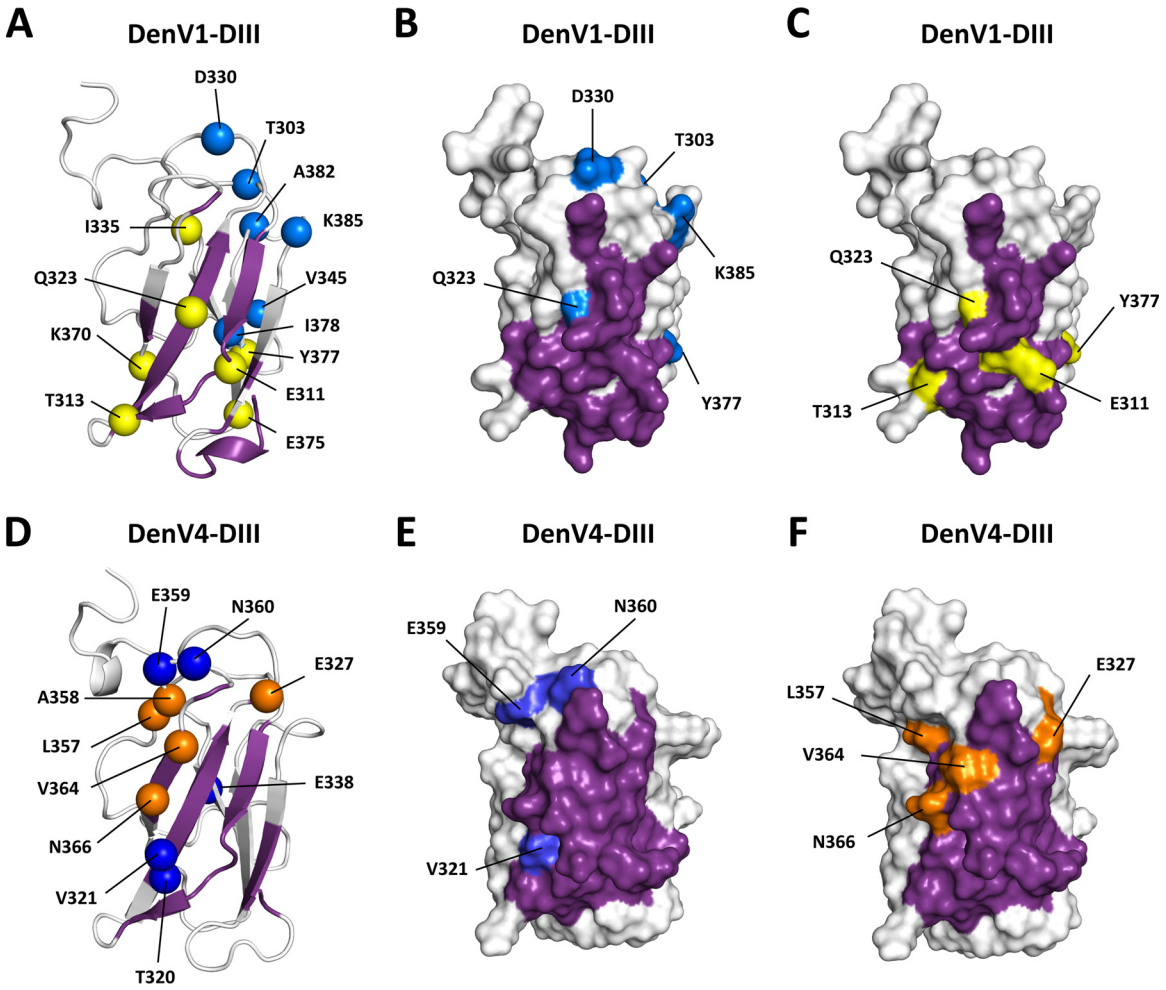

FIG 3 Effect of antibody binding on antigen flexibility. Shown are cartoon and surface representations of DIII-1 (A to C) and DIII-4 (D to F). The epitope of antibody DV32.6 is shown in purple, as described in the legends of Fig. 1 and 2. Residues showing conformational exchange in the free antigen are in dark and light blue, as described in the Fig. 1 and 2 legends. Residues showing conformational exchange only when the antigen is bound by the antibody are shown in yellow and orange. In DIII-4 (bottom), the conformational exchange of epitope residues (blue) is eliminated by antibody binding in a process suggestive of conformational selection. Binding, however, causes conformational exchange in different antigen residues (orange), suggesting that antibody binding can alter the antigen structure. A similar pattern can be detected in DIII-1, but the residues involved are different.

rigid upon complex formation. Conversely, CDR loops that are already rigid might bind antigens with higher affinity and specificity. Indeed, one view is that naive antibodies might be flexible and capable of recognizing a diverse antigen repertoire with low affinity. After maturation, instead, the CDR loops might become rigid, specific, and highly effective, with binding affinity often reaching subnanomolar levels.

One question, however, is how high-affinity antibodies can interact with flexible antigen regions. Does the antigen alternate between different conformations, one of which is selected by the antibody? Does the antigen become rigid upon complex formation, carrying an entropic cost presumably compensated for by the formation of favorable intermolecular interactions (52, 53)?

Here we investigated the interaction of human antibody DV32.6, which binds to the four existing dengue virus serotypes with nanomolar affinity, and domain III of E, the surface protein of dengue virus.

Dengue virus E protein is a particularly relevant model to study antigen flexibility because molecular motions are critical for both the infection cycle (requiring conformational rearrangement involving DIII) and antibody recognition. On one hand, anti-DIII antibodies have been shown to bind to epitopes that are not accessible in the known structures of the virus, suggesting that molecular rearrangements are required to expose them (54, 55); on the other hand, antibody binding was shown to either alter the virus structure or trap the antigen in an already existing conformation (21).

As a first step, we measured the backbone flexibility of the isolated DIII of DENV serotypes 1 and 4 by ^{15}N relaxation solution NMR experiments. DIII-1 and DIII-4 showed very similar dynamics in the picosecond-to-nanosecond time scale, which is sensitive to reorientational movements of the NH bond and therefore characterizes the rotational diffusion and internal motions in the thermal energy range (39). Residues located in the N and C termini have higher mobility; the BC, CD, and EF loops also present a higher degree of flexibility than residues located in the β-strands. Contributions of movements in the microsecond-to-millisecond time scale, typically associated with motion and rearrangements of specific regions of the protein, are also visible.

However, it is worth mentioning here that DIII-1 and DIII-4 show many differences in dynamics in this time scale. It is tempting to think that such differences might have an effect on antibody recognition of different serotypes. A cross-reactive antibody, in other words, might have to adapt not only to different primary sequences but also to different dynamic behaviors of the antigen.

In DIII-1, nine residues contribute to conformational exchange in the microsecond-to-millisecond time scale (Fig. 1B). None of these residues is involved in conformational exchange in DIII-4, where 5 other residues are in conformational exchange (Fig. 1B). These residues are part of the epitope of antibody DV32.6, discussed below, but are also close to residues that form interdomain interactions critical for the stability of the E protein dimers on the virus surface.

Residue H317, for instance, triggers the conformational changes induced by pH variation after cell entry, when the salt bridge between E368 and R9 is replaced by the salt bridge E368-H317 in the low-pH endosomal environment (8, 11, 56, 57). The resulting disruption of the interdomain interactions leads to the separation of DIII and rearrangement of the E protein from a dimeric to a trimeric conformation. The NMR-observed movement regime and conformational exchange of the β-strand might influence the position of H317 and its interdomain interactions, facilitating the movement of DIII which is required for the low-pH-induced conformation and to expose the epitope of DV32.6 and other antibodies on the virus surface. Interestingly, in DIII-4, H390 is close to E186 located in DI of another E protein dimer on the virus surface. Protonation of this histidine at endosomal pH might strengthen the interaction through the formation of electrostatic contacts. The histidine is not conserved in other serotypes, suggesting that disruption of the E protein arrangement might be more readily achieved.

Antibody DV32.6 (see below) has the peculiarity of binding strongly to its epitope on the isolated domain III of dengue virus serotype 4 (equilibrium dissociation constant [K_D] of 34 nM) but fails to effectively neutralize this serotype. In contrast, binding to DIII-1 is weaker (K_D of 145 nM), but this serotype is neutralized by the antibody (50% inhibitory concentration [IC_{50}] of 4 μg/ml). It is possible that, thanks to the above-mentioned dynamic differences, in the context of the full virus, the DV32.6 epitope is more readily accessible on dengue virus serotype 1 than on dengue virus serotype 4.

The impact of antibody binding on the structure and dynamics of DIII-1 and DIII-4 was also assessed by NMR spectroscopy. Most of the DIII epitope residues, identified by both chemical shift perturbation analysis and accessibility to a paramagnetic probe, are located in the patch formed by β-strands A, B, and D. When these residues are analyzed in the context of the full E protein crystal structures, it is evident that the majority of the epitope is covered by other domains of the E protein dimer (Fig. 2). Similarly, the epitopes of all other anti-DIII antibodies with a known structure are partially inaccessible on the virus surface (1A1D-2, 4E11, and 2H12) (20, 54, 55). Conformational changes causing different degrees of epitope exposure are likely important for the binding, specificity, and neutralization capacities of antibodies against the four different serotypes (20, 27, 58).

We obtained a quantitative description of the backbone dynamics of DIII in the presence of scFv antibody DV32.6. The values for the relaxation parameters and for the R_2/R_1 ratio of the complex are much higher than those of free DIII-1 and DIII-4, as expected for a complex with a molecular mass of ~35 kDa. Binding of scFv DV32.6 to DIII-1 leads to changes in conformational exchange mainly in the microsecond-to-millisecond time scale. Residues that show conformational exchange in free DIII do not do so in the DIII-antibody complex. This is in line with the idea that antibody binding can contribute to conformational selection in DIII, with epitope residues becoming more rigid due to direct interactions with antibody residues.

Other DIII residues, however, are affected by conformational exchange even in the antibody-antigen complex. Furthermore, the residues in exchange occupy different regions of the domain: whereas they are spread in both the ABD and CEF β-sheets in DIII-1, the residues are clustered on one side of the ABD sheet in DIII-4. Part of the epitopes of both serotypes is in conformational exchange in the complex. One possible explanation for this is that the antibody needs to adapt to different serotypes and thus fails to form "ideal" contacts with some of the residues, resulting in exchange between alternate antigen conformations. For example, the antibody might be able to establish particularly favorable contacts with E311 in DIII-4 but not DIII-1 (Fig. 3, yellow). Conversely, residue N366 might not form specific interactions with the antibody in DIII-4 (Fig. 3, orange) but might do so in DIII-1. It is worth mentioning that the binding affinities for the two serotypes are similar but not identical, with K_D values of 34 nM for DIII-4 and 145 nM for DIII-1 for the full antibody. More surprisingly, other DIII-4 residues (E327, L357, A358, V364, and N366) that have no conformational exchange in the free protein show exchange after antibody binding.

Intermolecular contacts between antibody and epitope atoms alter the degree of freedom available to the latter, resulting in a change in dynamics. The antibody contributes to making the antigen more rigid at the binding site but actually allosterically increases its flexibility in other regions. At the biophysical level, this might lessen the entropic requirements of antibody binding, since the penalty attached to increased epitope rigidity is relieved by increased flexibility elsewhere. At the biological level, this suggests that the antibody can alter the structure and dynamics of DIII. This allosteric effect might contribute to the disruption of the intermolecular packing interactions on the DENV surface, resulting in an altered virus conformation, as seen by cryo-EM for antibody 1A1D-2 (20). The ability of DV32.6 and other DIII antibodies to neutralize DENV might arise from such a disruption of virus surface packing, resulting in virus inactivation.

Domain III contains epitopes for neutralizing antibodies and also participates in primary and secondary cell receptor recognition (59). High-pH-induced interdomain rearrangements involving DIII are required for virus fusion to the host membrane. DIII is also a target for the development of vaccines and antiviral agents. Although recent works have suggested that anti-DIII antibodies are rare and not crucial for the natural immune response to DENV (60, 61), they are relevant candidates for passive immunization therapies. Regardless of biomedical interest, DIII remains a good model for the study of antibody recognition and selectivity, also thanks to the existence of four main DENV serotypes. Many studies have provided extensive structural information on E protein and particularly on DIII, also in complex with antibodies. In contrast, there is very scarce information regarding the molecular dynamics of free DIII, and nothing is available on the dynamic effect of antibody binding, especially at the quantitative level.

In this work, we addressed various structural aspects of DIII and their importance for the dengue virus infection mechanism

and antibody recognition. We provided a dynamic description of free DIII, at physiological and endosomal pHs and in complex with human antibody DV32.6, which binds to DIII with nanomolar affinity. We observed conformational exchange in the isolated DIII, in regions important for the packing of E protein dimers on the virus surface. The relative lack of conformational stability is likely to facilitate the partial detachment of DIII from the other E protein domains, which is required to achieve fusion to the host cellular membranes and to expose the epitopes of various anti-DIII antibodies. Antibody binding not only removed the exchange regime in the epitope region, in a process reminiscent of conformational selection, but, somewhat surprisingly, also caused exchange in other parts of DIII through allosteric effects.

Protein flexibility is known to play important roles in both structure and intermolecular interactions. However, its role in antibody binding is often neglected. One reason for this is that quantitative dynamic information is very difficult to obtain through X-ray crystallography, the technique of choice for the characterization of antibody-antigen complexes. In contrast, solution NMR spectroscopy is perfectly suited to the study of molecular dynamics and transient structural conformations. This work provides one of the very rare descriptions of the effect of antibody binding on antigen flexibility.

ACKNOWLEDGMENTS

We are grateful to Antonio Lanzavecchia and Davide Corti for fruitful discussion about dengue virus. We also thank Karen Santos and Gileno Santos for valuable assistance.

This study was supported by the Brazilian and Swiss agencies CNPq (Joint Research Project Funding Brazil-Switzerland [590124/2011-0, BPPq-303785/2014-4, and 301407/2010-0]), FAPERJ (CNE E-26/102.747/2012, Tematicos E-26/110.090/2013, and Sediadas E-26/010.002905/2014), and INCT-INBEB; L.V., M.P., and L.S. acknowledge support by the BSJRP (2013) (SNF-138518 and KTI-15524.1).

A.H.M., L.V., and A.P.V. conceived of the study. L.S. and M.P. produced labeled DIII and scFv. A.H.M. and A.P.V. collected the NMR data and processed the spectra. All authors critically contributed to the analysis and interpretation of the data. A.H.M., L.V., and A.P.V. wrote the paper with contributions from the rest of the authors.

FUNDING INFORMATION

Brazilian Swiss Joint Research Programme (BSJRP) provided funding to Luca Varani under grant number 0112-04. Instituto Nacional de Ciência e Tecnologia em Biologia Estrutural e Bioimagem provided funding to Ana Paula Valente. MCTI | Conselho Nacional de Desenvolvimento Científico e Tecnológico (CNPq) provided funding to Ana Paula Valente under grant number 590124/2011-0. MCTI | Conselho Nacional de Desenvolvimento Científico e Tecnológico (CNPq) provided funding to Ana Paula Valente under grant numbers 303785/2014-4 and 301407/2010-0. Fundação Carlos Chagas Filho de Amparo à Pesquisa do Estado do Rio de Janeiro (FAPERJ) provided funding to Ana Paula Valente under grant numbers CNE- E-26/102.747/2012 and E-26/110.090/2013. Schweizerischer Nationalfonds zur Förderung der Wissenschaftlichen Forschung (SNF) provided funding to Luca Varani under grant number 138518.

REFERENCES

1. **Mukhopadhyay S, Kuhn RJ, Rossmann MG.** 2005. A structural perspective of the flavivirus life cycle. Nat Rev Microbiol **3:**13–22. http://dx.doi.org/10.1038/nrmicro1067.
2. **WHO.** 2009. Dengue: guidelines for diagnosis, treatment, prevention, and control. WHO, Geneva, Switzerland.
3. **Dejnirattisai W, Jumnainsong A, Onsirisakul N, Fitton P, Vasanawathana S, Limpitikul W, Puttikhunt C, Edwards C, Duangchinda T, Supasa S, Chawansuntati K, Malasit P, Mongkolsapaya J, Screaton G.** 2010. Cross-reacting antibodies enhance dengue virus infection in humans. Science **328:**745–748. http://dx.doi.org/10.1126/science.1185181.
4. **Gandham SHA, Volk DE, Lokesh GLR, Neerathilingam M, Gorenstein DG.** 2014. Thioaptamers targeting dengue virus type-2 envelope protein domain III. Biochem Biophys Res Commun **453:**309–315. http://dx.doi.org/10.1016/j.bbrc.2014.09.053.
5. **Lee YR, Liu MT, Lei HY, Liu CC, Wu JM, Tung YC, Lin YS, Yeh TM, Chen SH, Liu HS.** 2006. MCP1, a highly expressed chemokine in dengue haemorrhagic fever/dengue shock syndrome patients, may cause permeability change, possibly through reduced tight junctions of vascular endothelium cells. J Gen Virol **87:**3623–3630. http://dx.doi.org/10.1099/vir.0.82093-0.
6. **Chen Y, Maguire T, Hileman RE, Fromm JR, Esko JD, Linhardt RJ, Marks RM.** 1997. Dengue virus infectivity depends on envelope protein binding to target cell heparan sulfate. Nat Med **3:**866–871. http://dx.doi.org/10.1038/nm0897-866.
7. **Zhang Y, Zhang W, Ogata S, Clements D, Strauss JH, Baker TS, Kuhn RJ, Rossmann MG.** 2004. Conformational changes of the flavivirus E glycoprotein. Structure **12:**1607–1618. http://dx.doi.org/10.1016/j.str.2004.06.019.
8. **Modis Y, Ogata S, Clements D, Harrison SC.** 2004. Structure of the dengue virus envelope protein after membrane fusion. Nature **427:**313–319. http://dx.doi.org/10.1038/nature02165.
9. **Nayak V, Dessau M, Kucera K, Anthony K, Ledizet M, Modis Y.** 2009. Crystal structure of dengue virus type 1 envelope protein in the postfusion conformation and its implications for membrane fusion. J Virol **83:**4338–4344. http://dx.doi.org/10.1128/JVI.02574-08.
10. **Fibriansah G, Ng T-S, Kostyuchenko VA, Lee J, Lee S, Wang J, Lok S-M.** 2013. Structural changes in dengue virus when exposed to a temperature of 37°C. J Virol **87:**7585–7592. http://dx.doi.org/10.1128/JVI.00757-13.
11. **Modis Y, Ogata S, Clements D, Harrison SC.** 2003. A ligand-binding pocket in the dengue virus envelope glycoprotein. Proc Natl Acad Sci U S A **100:**6986–6991. http://dx.doi.org/10.1073/pnas.0832193100.
12. **Elahi M, Islam MM, Noguchi K, Yohda M, Kuroda Y.** 2013. High resolution crystal structure of dengue-3 envelope protein domain III suggests possible molecular mechanisms for serospecific antibody recognition. Proteins **81:**1090–1095. http://dx.doi.org/10.1002/prot.24237.
13. **Zhang X, Ge P, Yu X, Brannan JM, Bi G, Zhang Q, Schein S, Zhou ZH.** 2013. Cryo-EM structure of the mature dengue virus at 3.5-Å resolution. Nat Struct Mol Biol **20:**105–110. http://dx.doi.org/10.1038/nsmb.2463.
14. **Volk DE, Lee Y-C, Li X, Thiviyanathan V, Gromowski GD, Li L, Lamb AR, Beasley DWC, Barrett ADT, Gorenstein DG.** 2007. Solution structure of the envelope protein domain III of dengue-4 virus. Virology **364:**147–154. http://dx.doi.org/10.1016/j.virol.2007.02.023.
15. **Crill WD, Roehrig JT, Roehrig JT.** 2001. Monoclonal antibodies that bind to domain III of dengue virus E glycoprotein are the most efficient blockers of virus adsorption to Vero cells. J Virol **75:**7769–7773. http://dx.doi.org/10.1128/JVI.75.16.7769-7773.2001.
16. **Wahala WMPB, Kraus AA, Haymore LB, Accavitti-Loper MA, de Silva AM.** 2009. Dengue virus neutralization by human immune sera: role of envelope protein domain III-reactive antibody. Virology **392:**103–113. http://dx.doi.org/10.1016/j.virol.2009.06.037.
17. **Beltramello M, Williams KL, Simmons CP, Macagno A, Simonelli L, Quyen NTH, Sukupolvi-Petty S, Navarro-Sanchez E, Young PR, de Silva AM, Rey FA, Varani L, Whitehead SS, Diamond MS, Harris E, Lanzavecchia A, Sallusto F.** 2010. The human immune response to dengue virus is dominated by highly cross-reactive antibodies endowed with neutralizing and enhancing activity. Cell Host Microbe **8:**271–283. http://dx.doi.org/10.1016/j.chom.2010.08.007.
18. **Deng YQ, Dai JX, Ji GH, Jiang T, Wang HJ, Yang HO, Tan WL, Liu R, Yu M, Ge BX, Zhu QY, Qin De E, Guo YJ, Qin CF.** 2011. A broadly flavivirus cross-neutralizing monoclonal antibody that recognizes a novel epitope within the fusion loop of E protein. PLoS One **6:**e16059. http://dx.doi.org/10.1371/journal.pone.0016059.
19. **Watterson D, Kobe B, Young PR.** 2012. Residues in domain III of the dengue virus envelope glycoprotein involved in cell-surface glycosaminoglycan binding. J Gen Virol **93:**72–82. http://dx.doi.org/10.1099/vir.0.037317-0.
20. **Lok S-M, Kostyuchenko V, Nybakken GE, Holdaway HA, Battisti AJ, Sukupolvi-Petty S, Sedlak D, Fremont DH, Chipman PR, Roehrig JT, Diamond MS, Kuhn RJ, Rossmann MG.** 2008. Binding of a neutralizing

antibody to dengue virus alters the arrangement of surface glycoproteins. Nat Struct Mol Biol **15:**312–317. http://dx.doi.org/10.1038/nsmb.1382.
21. **Aoki C, Hidari KIPJ, Itonori S, Yamada A, Takahashi N, Kasama T, Hasebe F, Islam MA, Hatano K, Matsuoka K, Taki T, Guo CT, Takahashi T, Sakano Y, Suzuki T, Miyamoto D, Sugita M, Terunuma D, Morita K, Suzuki Y.** 2006. Identification and characterization of carbohydrate molecules in mammalian cells recognized by dengue virus type 2. J Biochem **139:**607–614. http://dx.doi.org/10.1093/jb/mvj067.
22. **Bai F, Town T, Pradhan D, Cox J, Ashish Ledizet M, Anderson JF, Flavell RA, Krueger JK, Koski RA, Fikrig E.** 2007. Antiviral peptides targeting the West Nile virus envelope protein. J Virol **81:**2047–2055. http://dx.doi.org/10.1128/JVI.01840-06.
23. **Hidari KIPJ, Takahashi N, Arihara M, Nagaoka M, Morita K, Suzuki T.** 2008. Structure and anti-dengue virus activity of sulfated polysaccharide from a marine alga. Biochem Biophys Res Commun **376:**91–95. http://dx.doi.org/10.1016/j.bbrc.2008.08.100.
24. **Marks RM, Lu H, Sundaresan R, Toida T, Suzuki A, Imanari T, Hernáiz MJ, Linhardt RJ.** 2001. Probing the interaction of dengue virus envelope protein with heparin: assessment of glycosaminoglycan-derived inhibitors. J Med Chem **44:**2178–2187. http://dx.doi.org/10.1021/jm000412i.
25. **Wang QY, Patel SJ, Vangrevelinghe E, Hao YX, Rao R, Jaber D, Schul W, Gu F, Heudi O, Ngai LM, Mee KP, Wai YP, Keller TH, Jacoby E, Vasudevan SG.** 2009. A small-molecule dengue virus entry inhibitor. Antimicrob Agents Chemother **53:**1823–1831. http://dx.doi.org/10.1128/AAC.01148-08.
26. **Yennamalli R, Subbarao N, Kampmann T, McGeary RP, Young PR, Kobe B.** 2009. Identification of novel target sites and an inhibitor of the dengue virus E protein. J Comput Aided Mol Des **23:**333–341. http://dx.doi.org/10.1007/s10822-009-9263-6.
27. **Simonelli L, Pedotti M, Beltramello M, Livoti E, Calzolai L, Sallusto F, Lanzavecchia A, Varani L.** 2013. Rational engineering of a human anti-dengue antibody through experimentally validated computational docking. PLoS One **8:**e55561. http://dx.doi.org/10.1371/journal.pone.0055561.
28. **Delaglio F, Grzesiek S, Vuister GW, Zhu G, Pfeifer J, Bax A.** 1995. NMRPipe: a multidimensional spectral processing system based on UNIX pipes. J Biomol NMR **6:**277–293. http://dx.doi.org/10.1007/BF00197809.
29. **Vranken WF, Boucher W, Stevens TJ, Fogh RH, Pajon A, Llinas M, Ulrich EL, Markley JL, Ionides J, Laue ED.** 2005. The CCPN data model for NMR spectroscopy: development of a software pipeline. Proteins **59:**687–696. http://dx.doi.org/10.1002/prot.20449.
30. **Farrow NA, Muhandiram R, Singer AU, Pascal SM, Kay CM, Gish G, Shoelson SE, Pawson T, Forman-Kay JD, Kay LE.** 1994. Backbone dynamics of a free and phosphopeptide-complexed Src homology 2 domain studied by 15N NMR relaxation. Biochemistry **33:**5984–6003. http://dx.doi.org/10.1021/bi00185a040.
31. **Kay LE, Torchia DA, Bax A.** 1989. Backbone dynamics of proteins as studied by 15N inverse detected heteronuclear NMR spectroscopy: application to staphylococcal nuclease. Biochemistry **28:**8972–8979. http://dx.doi.org/10.1021/bi00449a003.
32. **Barbato G, Ikura M, Kay LE, Pastor RW, Bax A.** 1992. Backbone dynamics of calmodulin studied by 15N relaxation using inverse detected two-dimensional NMR spectroscopy: the central helix is flexible. Biochemistry **31:**5269–5278.
33. **Farrow NA, Zhang O, Szabo A, Torchia DA, Kay LE.** 1995. Spectral density function mapping using 15N relaxation data exclusively. J Biomol NMR **6:**153–162.
34. **Lefevre JF, Dayie KT, Peng JW, Wagner G.** 1996. Internal mobility in the partially folded DNA binding and dimerization domains of GAL4: NMR analysis of the N-H spectral density functions. Biochemistry **35:**2674–2686. http://dx.doi.org/10.1021/bi9526802.
35. **d'Auvergne EJ, Gooley PR.** 2008. Optimisation of NMR dynamic models. II. A new methodology for the dual optimisation of the model-free parameters and the Brownian rotational diffusion tensor. J Biomol NMR **40:**121–133.
36. **d'Auvergne EJ, Gooley PR.** 2008. Optimisation of NMR dynamic models. I. Minimisation algorithms and their performance within the model-free and Brownian rotational diffusion spaces. J Biomol NMR **40:**107–119.
37. **Lipari G, Szabo A.** 1982. Model-free approach to the interpretation of nuclear magnetic resonance relaxation in macromolecules. 2. Analysis of experimental results. J Am Chem Soc **104:**4559–4570. http://dx.doi.org/10.1021/ja00381a010.
38. **Dosset P, Hus JC, Blackledge M, Marion D.** 2000. Efficient analysis of macromolecular rotational diffusion from heteronuclear relaxation data. J Biomol NMR **16:**23–28. http://dx.doi.org/10.1023/A:1008305808620.
39. **Palmer AG, Massi F.** 2006. Characterization of the dynamics of biomacromolecules using rotating-frame spin relaxation NMR spectroscopy. Chem Rev **106:**1700–1719. http://dx.doi.org/10.1021/cr0404287.
40. **Palmer AG, III.** 2004. NMR characterization of the dynamics of biomacromolecules. Chem Rev **104:**3623–3640. http://dx.doi.org/10.1021/cr030413t.
41. **Carr HY, Purcell EM.** 1954. Effects of diffusion on free precession in nuclear magnetic resonance experiments. Phys Rev **94:**630–638. http://dx.doi.org/10.1103/PhysRev.94.630.
42. **Meiboom S, Gill D.** 1958. Modified spin-echo method for measuring nuclear relaxation times. Rev Sci Instrum **29:**688–691. http://dx.doi.org/10.1063/1.1716296.
43. **Korzhnev DM, Kay LE.** 2008. Probing invisible, low-populated states of protein molecules by relaxation dispersion NMR spectroscopy: an application to protein folding. Acc Chem Res **41:**442–451. http://dx.doi.org/10.1021/ar700189y.
44. **Mittermaier AK, Kay LE.** 2009. Observing biological dynamics at atomic resolution using NMR. Trends Biochem Sci **34:**601–611. http://dx.doi.org/10.1016/j.tibs.2009.07.004.
45. **Kovrigin EL, Kempf JG, Grey MJ, Loria JP.** 2006. Faithful estimation of dynamics parameters from CPMG relaxation dispersion measurements. J Magn Reson **180:**93–104. http://dx.doi.org/10.1016/j.jmr.2006.01.010.
46. **Prakash MK, Barducci A, Parrinello M.** 2010. Probing the mechanism of pH-induced large-scale conformational changes in dengue virus envelope protein using atomistic simulations. Biophys J **99:**588–594. http://dx.doi.org/10.1016/j.bpj.2010.04.024.
47. **Zhang X, Sheng J, Austin SK, Hoornweg TE, Smit JM, Kuhn RJ, Diamond MS, Rossmann MG.** 2015. Structure of acidic pH dengue virus showing the fusogenic glycoprotein trimers. J Virol **89:**743–750. http://dx.doi.org/10.1128/JVI.02411-14.
48. **Bardelli M, Livoti E, Simonelli L, Pedotti M, Moraes A, Valente AP, Varani L.** 2015. Epitope mapping by solution NMR spectroscopy. J Mol Recognit **28:**393–400. http://dx.doi.org/10.1002/jmr.2454.
49. **Pintacuda G, Otting G.** 2002. Identification of protein surfaces by NMR measurements with a paramagnetic Gd(III) chelate. J Am Chem Soc **124:**372–373. http://dx.doi.org/10.1021/ja016985h.
50. **Eisenmesser EZ, Millet O, Labeikovsky W, Korzhnev DM, Wolf-Watz M, Bosco DA, Skalicky JJ, Kay LE, Kern D.** 2005. Intrinsic dynamics of an enzyme underlies catalysis. Nature **438:**117–121. http://dx.doi.org/10.1038/nature04105.
51. **Neudecker P, Lundström P, Kay LE.** 2009. Relaxation dispersion NMR spectroscopy as a tool for detailed studies of protein folding. Biophys J **96:**2045–2054. http://dx.doi.org/10.1016/j.bpj.2008.12.3907.
52. **James LC, Tawfik DS.** 2005. Structure and kinetics of a transient antibody binding intermediate reveal a kinetic discrimination mechanism in antigen recognition. Proc Natl Acad Sci U S A **102:**12730–12735. http://dx.doi.org/10.1073/pnas.0500909102.
53. **Adhikary R, Yu W, Oda M, Zimmermann J, Romesberg FE.** 2012. Protein dynamics and the diversity of an antibody response. J Biol Chem **287:**27139–27147. http://dx.doi.org/10.1074/jbc.M112.372698.
54. **Cockburn JJB, Navarro Sanchez ME, Fretes N, Urvoas A, Staropoli I, Kikuti CM, Coffey LL, Arenzana Seisdedos F, Bedouelle H, Rey FA.** 2012. Mechanism of dengue virus broad cross-neutralization by a monoclonal antibody. Structure **20:**303–314. http://dx.doi.org/10.1016/j.str.2012.01.001.
55. **Midgley CM, Flanagan A, Tran HB, Dejnirattisai W, Chawansuntati K, Jumnainsong A, Wongwiwat W, Duangchinda T, Mongkolsapaya J, Grimes JM, Screaton GR.** 2012. Structural analysis of a dengue cross-reactive antibody complexed with envelope domain III reveals the molecular basis of cross-reactivity. J Immunol **188:**4971–4979. http://dx.doi.org/10.4049/jimmunol.1200227.
56. **Li L, Lok S-M, Yu I-M, Zhang Y, Kuhn RJ, Chen J, Rossmann MG.** 2008. The flavivirus precursor membrane-envelope protein complex: structure and maturation. Science **319:**1830–1834. http://dx.doi.org/10.1126/science.1153263.
57. **Fritz R, Stiasny K, Heinz FX.** 2008. Identification of specific histidines as pH sensors in flavivirus membrane fusion. J Cell Biol **183:**353–361. http://dx.doi.org/10.1083/jcb.200806081.
58. **Gromowski GD, Barrett ND, Barrett ADT.** 2008. Characterization of dengue virus complex-specific neutralizing epitopes on envelope protein

domain III of dengue 2 virus. J Virol **82:**8828–8837. http://dx.doi.org/10.1128/JVI.00606-08.

59. **Lisova O, Belkadi L, Bedouelle H.** 2014. Direct and indirect interactions in the recognition between a cross-neutralizing antibody and the four serotypes of dengue virus. J Mol Recognit **27:**205–214. http://dx.doi.org/10.1002/jmr.2352.
60. **Rouvinski A, Guardado-Calvo P, Barba-Spaeth G, Duquerroy S, Vaney M-C, Kikuti CM, Navarro Sanchez ME, Dejnirattisai W, Wongwiwat W, Haouz A, Girard-Blanc C, Petres S, Shepard WE, Desprès P, Arenzana-Seisdedos F, Dussart P, Mongkolsapaya J, Screaton GR, Rey FA.** 2015. Recognition determinants of broadly neutralizing human antibodies against dengue viruses. Nature **520:**109–113. http://dx.doi.org/10.1038/nature14130.
61. **Dejnirattisai W, Wongwiwat W, Supasa S, Zhang X, Dai X, Rouvinsky A, Jumnainsong A, Edwards C, Quyen NTH, Duangchinda T, Grimes JM, Tsai W, Lai C, Wang W, Malasit P, Farrar J, Simmons CP, Zhou ZH, Rey FA, Mongkolsapaya J, Screaton GR.** 2015. A new class of highly potent, broadly neutralizing antibodies isolated from viremic patients infected with dengue virus. Nat Immunol **16:**170–177. http://dx.doi.org/10.1038/ni.3058.